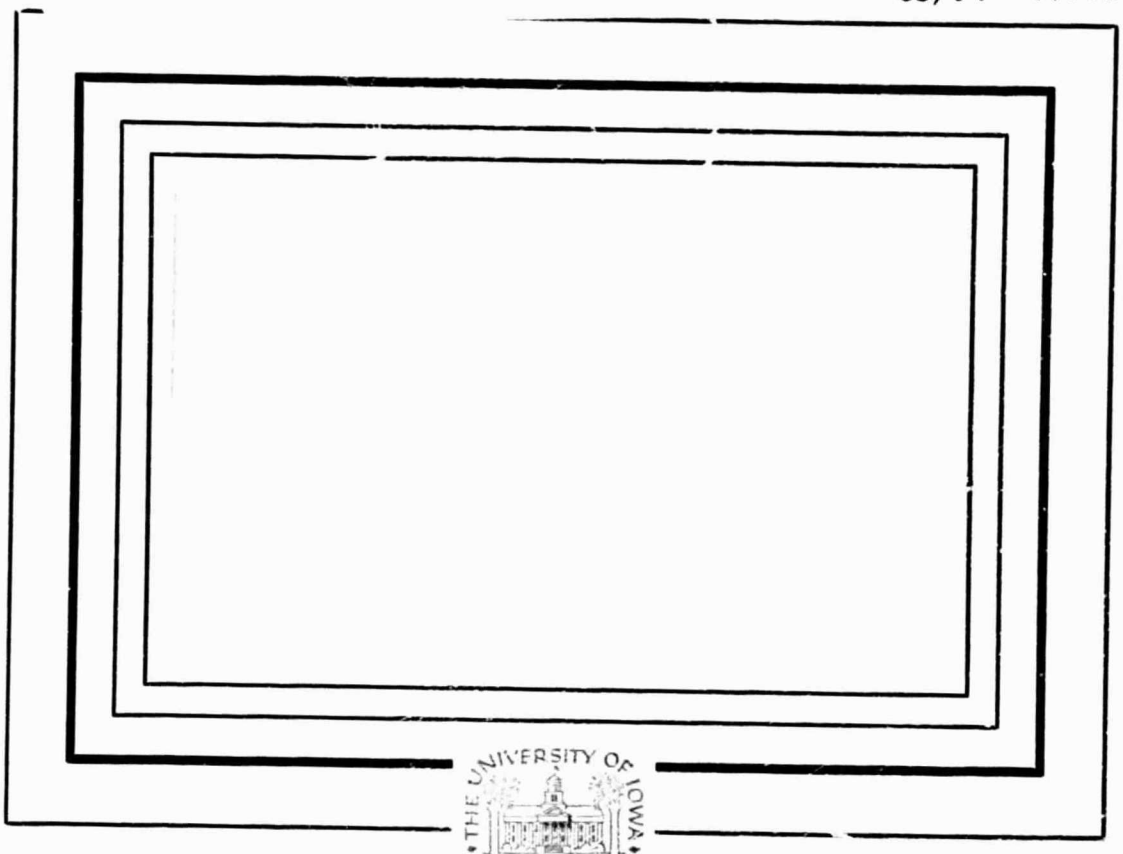

Department of Physics and Astronomy

THE UNIVERSITY OF IOWA

Iowa City, Iowa 52242

U. of Iowa 81-3

Plasma Waves near Saturn:

Initial Results from Voyager 1

by

D. A. Gurnett[1], W. S. Kurth[1],

and F. L. Scarf[2]

January, 1981

[1]Department of Physics and Astronomy, The University of Iowa, Iowa City, Iowa 52242

[2]Space Sciences Department, TRW Defense and Space Systems Group, Redondo Beach, California 90278

The research at The University of Iowa was supported by NASA through contract 954013 with JPL, through grants NGL-16-001-002 and NGL-16-001-043 with NASA Headquarters and by the Office of Naval Research. The research at TRW was supported by NASA through contract 954012 with JPL.

UNCLASSIFIED

SECURITY CLASSIFICATION OF THIS PAGE (When Data Entered)

REPORT DOCUMENTATION PAGE		READ INSTRUCTIONS BEFORE COMPLETING FORM
1. REPORT NUMBER U. of Iowa 81-3	2. GOVT ACCESSION NO.	3. RECIPIENT'S CATALOG NUMBER
4. TITLE (and Subtitle) PLASMA WAVES NEAR SATURN: INITIAL RESULTS FROM VOYAGER 1		5. TYPE OF REPORT & PERIOD COVERED Progress January 1981 6. PERFORMING ORG. REPORT NUMBER
7. AUTHOR(s) D. A. GURNETT, W. S. KURTH, and F. L. SCARF		8. CONTRACT OR GRANT NUMBER(s) N00014-76-C-0016
9. PERFORMING ORGANIZATION NAME AND ADDRESS Department of Physics and Astronomy The University of Iowa Iowa City, Iowa 52242		10. PROGRAM ELEMENT, PROJECT, TASK AREA & WORK UNIT NUMBERS
11. CONTROLLING OFFICE NAME AND ADDRESS Office of Naval Research Electronics Program Office Arlington, Virginia 22217		12. REPORT DATE 31 January 1981 13. NUMBER OF PAGES 28
14. MONITORING AGENCY NAME & ADDRESS(if different from Controlling Office)		15. SECURITY CLASS. (of this report) UNCLASSIFIED 15a. DECLASSIFICATION/DOWNGRADING SCHEDULE

16. DISTRIBUTION STATEMENT (of this Report)

Approved for public release; distribution is unlimited.

17. DISTRIBUTION STATEMENT (of the abstract entered in Block 20, if different from Report)

18. SUPPLEMENTARY NOTES

To be published in Science, 1981

19. KEY WORDS (Continue on reverse side if necessary and identify by block number)

Plasma Waves
Saturn

20. ABSTRACT (Continue on reverse side if necessary and identify by block number)

(See page following)

DD FORM 1 JAN 73 1473 EDITION OF 1 NOV 65 IS OBSOLETE
S/N 0102-014-6601

UNCLASSIFIED

SECURITY CLASSIFICATION OF THIS PAGE (When Data Entered)

Abstract. The Voyager 1 plasma wave instrument detected many familiar types of plasma waves during the encounter with Saturn, including ion-acoustic waves and electron plasma oscillations upstream of the bow shock, an intense burst of electrostatic noise at the shock, and chorus, hiss, electrostatic $(n + 1/2)f_g$ waves and UHR emissions in the inner magnetosphere. A clock-like Saturn rotational control of low-frequency radio emissions was observed, and evidence was obtained of possible control by the moon Dione. Strong plasma wave emissions were detected at the Titan encounter indicating the presence of a turbulent sheath extending around Titan, and UHR measurements of the electron density show the existence of a dense plume of plasma being carried downstream of Titan by the interaction with the rapidly rotating magnetosphere of Saturn.

Introduction. The Voyager 1 encounter with Saturn in November 1980 has now provided the first opportunity to investigate plasma wave interactions in the magnetosphere of Saturn. This paper presents an overview of the principal results from the Voyager 1 plasma wave instrument starting with the initial detection of Saturn and ending about four weeks after closest approach. A survey plot of the electric field intensities detected during the Saturn encounter is shown in Figure 1, starting shortly before the inbound shock crossing and ending shortly after the outbound magnetopause crossing. As can be seen, many intense waves were observed in the vicinity of Saturn. To provide a framework for presenting the observations, the results are discussed more or less according to the sequence in which the data were obtained. The only exceptions are the Saturn radio emissions which are discussed last. For a detailed account of the design and operating characteristics of the Voyager plasma wave instrument, see the previous report by Scarf and Gurnett (1).

Upstream sola. wind, bow shock, and magnetopause. During the approach to Saturn the solar wind upstream of Saturn was remarkably quiet. Occasionally, when the proper magnetic connection was available to the bow shock, brief bursts of ion-acoustic waves were detected with characteristics similar to the ion-acoustic waves detected upstream of the Jovian bow shock (2). Saturn's bow shock, indicated by S in Figure 1, was encountered at 2327 spacecraft event time (SCET) on 11 November at a radial distance of 26.2 R_S. A brief burst of electron plasma oscillations occurred ahead of the shock followed by an intense burst of broadband electric field noise at the shock with characteristics very similar to the bow shock at Jupiter (2). Downstream of the shock the electric field intensities in the magnetosheath were very low. Five magnetopause crossings, indicated by M in Figure 1, were observed on the inbound pass with the first and last occurring at 0154 and 0248 on 12 November. At each magnetopause crossing a brief narrowband burst of electric field noise occurred in the 5.62-kHz channel, probably due to either electron plasma oscillations or upper hybrid resonance emissions. In the outer regions of the magnetosphere, the electric field intensities again returned to very low levels. No evidence was found for trapped continuum radiation comparable to that observed in the magnetospheres of Earth or Jupiter (2).

Titan encounter. One of the main targeting objectives of the Voyager 1 encounter with Saturn was a very close flyby of the moon Titan, which was inside the magnetosphere at the time of the encounter. The close flyby provided a good opportunity to study the interaction of Titan with the rapidly rotating magnetospheric plasma of Saturn,

which flows by at a nominal velocity of about 200 km/sec. Several major effects were observed in the plasma wave data near Titan. As shown in Figure 2, two regions of intense low-frequency electric-field turbulence were detected in the vicinity of Titan. The spectrum and qualitative characteristics of this turbulence are very similar to the electrostatic turbulence observed in the magnetosheath and ionosheath of Earth and Venus (3). These similarities suggest the existence of a highly turbulent sheath-like region extending around Titan as illustrated at the top of Figure 2. This turbulence is believed to consist of ion-acoustic waves driven by currents and non-equilibrium plasma distributions in the sheath. A pronounced asymmetry is evident in the thickness of the sheath and the spectrum of the noise on the inbound and outbound passes. Corresponding asymmetries with almost identical boundaries are also evident in the magnetic field signature reported by the Voyager magnetometer team (4). The initial intense burst of noise at 0532:30 suggests a shock-like interaction at the upstream boundary of the sheath. Although the flow is believed to be sub-Alfvenic, it is possible that the interaction could be a slow-mode shock.

At higher frequencies, above 5 kHz, a series of narrowband emissions can be seen sweeping through adjacent frequency channels. These emissions are identified by circles in Figure 2. Based on the close similarity to narrowband upper hybrid emissions observed in the magnetosphere at Earth (5), these emissions are believed to be at the local upper hybrid resonance (UHR) frequency, $f_{UHR} = \sqrt{f_p^2 + f_g^2}$, where f_p and f_g are the electron plasma frequency and gyrofrequency. Since $f_g << f_p$, the UHR emission frequency provides a direct determination of

the local electron density, $N = (f_p/9000)^2$ in cm^{-3}. Using the scale on the left of Figure 2, the smooth dashed line through the circled UHR emissions gives our initial determination of the electron density profile. These measurements show that the peak electron density in the wake of Titan, ~ 40 cm^{-3}, is several orders of magnitude larger than the electron density, ~ 0.01 to 0.1 cm^{-3}, in the surrounding magnetosphere. The high densities in the wake, the steep density gradients and the alignment of the density maximums with the sheath boundaries strongly suggest that the spacecraft has passed through a dense plume of plasma which is being swept away from Titan by the magnetospheric interaction. The density profile of the wake disturbance appears to be shifted about 10° to 20° toward Saturn with respect to the plasma flow expected for rigid corotation.

Coincident with the exit from the region of enhanced density an abrupt onset of radio emissions can be seen at about 0542:40 in the 56.2-kHz channel of Figure 2. The intensity of this radio emission gradually decreases to the instrument noise level over a 2-hour period after the Titan encounter (see Figure 1). Two interpretations of this radio emission have been proposed. The abrupt onset of the radiation at Titan and the gradual decrease in intensity with increasing radial distance from Titan seem to indicate that Titan is the source of this radiation. The source would then have to be on the Saturn-facing side of Titan as illustrated at the top of Figure 2. The occurrence of intense UHR emissions on the same side of Titan suggests that the generation mechanism may be the same as continuum radiation at Earth, which is believed to be generated by UHR emissions at the plasmapause (5). Since Saturn also emits radio noise in this same frequency range,

Saturn must also be considered as a possible source. If Saturn is the source then the abrupt onset at Titan could be a propagation cutoff caused by the high electron density near Titan. Although we have no results which can definitely eliminate Saturn as the source, examination of temporal fluctuations shows that the Titan associated radiation has characteristics which are quite different from the typical Saturn radio emissions.

Magnetosphere. Within the magnetosphere the greatest plasma wave activity occurs in the inner regions, inside of about 10 R_S. A detailed plot of the electric field intensities in the region near closest approach is shown in Figure 3. To interpret the plasma wave intensities it is necessary to know the electron gyrofrequency f_g and plasma frequency f_p. The electron gyrofrequency profile (f_g = 28 B in Hz, where B is the magnetic field in gammas) can be determined from the magnetic field measurements (4) and is shown by the solid line in Figure 3. The plasma frequency profile is more difficult to determine and must be obtained by a combination of interpretation and comparison with direct measurements (6). For example, the brief bursts of electron plasma oscillations from about 1800 to 2000 on 12 November show that the plasma frequency is between 10 and 17.8 kHz at these times. Continuing past 2000 a band of radio emission can be seen in the high-frequency channels with a well-defined low-frequency cutoff. The cutoff first decreases, reaches a minimum of about 3 kHz at 2300 on 12 November, and then increases to about 31.1 kHz at 0130 on 13 November, where an intense UHR emission occurs. This cutoff is believed to be at the electron plasma frequency, which represents the low-frequency limit of the free-space electromagnetic mode. Although the cutoff only provides an upper limit for the local plasma frequency,

comparisons with the electron densities from the plasma instrument (6) at a few isolated points show that the cutoff is very close to the local plasma frequency. The resulting plasma frequency contour is shown by the dashed line in Figure 3. After about 0200 on 13 November it becomes very difficult to determine the plasma frequency profile. The main indications are that it is near 31.1 kHz around 0500, because of the UHR emission at this time, and that after 0900 the plasma frequency again drops to a low value, 3 kHz or less, because of the high-frequency radio emissions which extend down into the 3.11-kHz channel after this time.

The interpretation of these plasma frequency variations is illustrated in Figure 4, which shows a meridian plane projection of the spacecraft trajectory. Two principal effects are noted, namely that the plasma frequency, hence electron density, is very low (< 1 cm^{-3}) from about 2030 on 12 November to 0100 on 13 November, and again after 0900 on 13 November. Assuming that the plasma density distribution is symmetric with respect to the rotational axis of Saturn, it is seen that these variations represent penetrations into low density regions north and south of a dense equatorially-confined plasma torus. In the central region of the torus the electron densities range from about 10 to 40 cm^{-3}, which are consistent with the Pioneer 11 measurements of Frank et al. (7). The north-south thickness of the torus is about 4 R_S.

Further identification of the plasma wave emissions in Figure 3 is greatly assisted by the 48-second frames of wideband waveform data obtained near closest approach. Figure 5 shows spectrograms of the wideband data obtained at points A and B in Figure 3. Spectrogram A was obtained at 2251:46 on 12 November, shortly before closest approach, and

spectrogram B was obtained at 0326:10 on 13 November, shortly before crossing the equatorial plane. Both spectrograms show the occurrence of a strong band of noise at frequencies below 2 kHz, in the frequency range appropriate for the whistler mode ($f \lesssim f_g$ and $f \lesssim f_p$). Spectrogram B shows that this noise consists of discrete tones and a relatively steady band of noise which closely resembles the whistler-mode chorus and hiss emissions observed in the terrestrial and Jovian magnetospheres (8). In spectrogram A the chorus is completely absent and the emission appears to consist entirely of hiss. The survey plot in Figure 3 shows that the whistler-mode emissions reach maximum intensity at about 0410 on 13 November, coincident with the equatorial plane crossing. Preliminary estimates indicate that the chorus and hiss emissions in this region are in resonance with electrons of relatively low energy, in the range from 1 to 5 keV.

Spectrogram B in Figure 5 shows another series of emissions slightly above f_g, $2f_g$, and $3f_g$. These emissions are electrostatic electron cyclotron waves of the type previously observed in both the terrestrial and Jovian magnetospheres (9). These emissions tend to occur near half-integral harmonics of the electron cyclotron frequency and are identified in Figure 3 as $(n + 1/2)f_g$ bands. Spectrogram A in Figure 5 shows a large number of puzzling bands. Several characteristic frequency spacings can be identified, including about 875 Hz, 1.45 kHz and 3.90 kHz. None of these band spacings are related to the local electron gyrofrequency, which is $f_g = 25.3$ kHz. These emissions are believed to be propagating in the free-space electromagnetic mode since they can be detected at the same frequency over a wide range of radial distances. In considering the origin of these narrowband electromagnetic emissions, we

suggest that the emissions are probably generated by conversion from electrostatic $(n + 1/2)f_g$ emissions near the upper hybrid resonance, similar to the generation of continuum radiation in the terrestrial magnetosphere (10). If the characteristic frequency spacings corresponds to the electron gyrofrequency in the plasma torus, then the emissions would originate from about 8.6, 7.3 and 5.2 R_S. It has occurred to us that these radial distances are close to the orbits of Rhea, Dione and Tethys, which suggests that these moons may be involved in the generation of the radio emissions.

Near closest approach we also carried out a search for lightning-generated whistlers. Many impulsive signals were detected near closest approach, some of which can be seen in spectrogram B of Figure 5. However, none of these signals appear to have dispersion characteristics consistent with whistlers generated by lightning in Saturn's atmosphere. The origin of these impulsive signals is still being investigated. Other possibilities being considered include Doppler-shifted ion-acoustic waves, electrostatic discharges on the spacecraft and spacecraft-generated interference.

During the outbound pass through the high latitude region of the magnetosphere, the intensities again returned to very low levels. No indication was found for intense low frequency continuum radiation of the type observed in the magnetotail of Jupiter (2). The main effect of interest in the high latitude magnetotail is the intense low frequency electric field noise evident in Figure 1 from about 1930 to 2400 on 13 November. This noise appears to be similar to the broadband electrostatic noise observed along the auroral field lines in the terrestrial magnetosphere (11). It is interesting to note that this noise also

occurs at L-values consistent with the observed location of the aurora at Saturn (12).

Saturn radio emissions. Several months before the Voyager 1 encounter with Saturn, the Planetary Radio Astronomy (PRA) team identified strong nonthermal radio emissions originating from Saturn's magnetosphere (13). These radio emissions are most intense in the kilometer wavelength range and are strongly controlled by the rotation of Saturn. The rotational period was determined to be 10 hr. 39.4 min. Because the peak in the emission spectrum occurs slightly above the frequency range of the plasma wave instrument, these radio emissions were not regularly detected in the plasma wave data until about six weeks before closest approach. Initially, the signals were only detected in the highest frequency channel. However, as the spacecraft approached Saturn the intensities increased rapidly and it became possible to detect the radio emissions at much lower frequencies, sometimes as low as 3 kHz. The top panel of Figure 6, for example, shows a typical radio event plotted over a time interval corresponding to one complete rotation. The time origin has been selected to correspond to the time when the sun is at 0° longitude in the Saturn Longitude System (SLS) defined Desch and Kaiser (13). As can be seen the emission is most intense in the highest, 56.2 kHz, channel and lasts for about one-half of a Saturn rotation with maximum intensity when the subsolar longitude is near 90°.

A basic question concerning the radio emission process is whether the rotational control is caused by a radiation pattern which rotates with the planet, like a rotating searchlight, or whether the modulation is a temporal effect, like a flashing light. These two models can

be tested by comparing the phase of the rotational modulation on the inbound and outbound passes. If the modulation is caused by the searchlight effect, the phase should shift by an amount corresponding to the angle between the inbound and outbound trajectories projected into the equatorial plane, which is about 135°. The rotational modulation for the inbound and outbound passes is illustrated in the bottom panel of Figure 6, which shows the probability of the radio emission intensity exceeding 1.9×10^{-18} W/m^2 Hz at 56.2 kHz as a function of the subsolar SLS longitude. As can be seen there is essentially no phase difference between the inbound and outbound passes. This result implies that the control is a temporal or clock-like effect, in which the radiation is emitted simultaneously over a wide range of directions at a particular phase of Saturn's rotation. Because of the very small tilt of the magnetic dipole axis of Saturn with respect to the rotational axis (14,4), the origin of this pronounced rotational control is difficult to understand. It is considered most likely, for example, that the modulation is caused by a high order distortion of the magnetic field near the planet, but the mechanism by which this distortion could affect the radio emission is not clear.

Although Saturn's rotation has a major effect on the radio emission process it is clear that other factors are also involved since the intensity of the events varies substantially on time scales of days. This long-term variability is illustrated in Figure 7, which shows a 16-day plot of the 56.2-kHz intensities centered on closest approach. In addition to the basic rotational control an overall modulation of the intensities can be seen with a period slightly less than 3 days. For instance, intense events are present on days 313, 316, 318-319, 321 and 324.

Because of the well-known control of Jovian radio emissions by the moon Io, an obvious explanation of this periodicity is that one of the moons of Saturn is influencing the radio emission process. The only moon with a suitable period is Dione, which has a period of 2.74 days. To explore this possibility, a plot of the orbital phase angle of Dione is shown in the bottom panel of Figure 7. As can be seen, the correlation appears to be quite good. A further analysis using all of the available data is illustrated in Figure 8, which shows the radio emission intensity at 56.2 kHz as a function of both the subsolar SLS longitude and the Dione orbital phase. The significance of the combined control by these two parameters is best seen by comparing the relative intensities in the upper-left and lower-right quadrants. It is evident that the largest radio emission intensities occur when the subsolar SLS longitude is near 90° and Dione is passing through the local morning region of the magnetosphere. The best correlation with Dione's position occurs during the few-week period around closest approach, when the intensities are largest.

The apparent control of the Saturnian radio emission intensities by Dione, suggests that this moon may be involved in a strong magnetospheric interaction, possibly similar to the interaction of Io with the Jovian magnetosphere. Most likely this interaction would imply outgassing and production of plasma by Dione, similar to the situation at Io. Although there is no evidence of volcanic activity, the photographs of Dione show white whispy features which indicate the loss of volatile material (15). Furthermore, the Pioneer 11 plasma measurements show a peak in the plasma density profile near Dione's orbit (7), suggesting that Dione is a source of plasma. If Dione is injecting plasma into the magnetosphere numerous

mechanisms could account for the dependence on orbital position, including magnetospheric dawn-dusk asymmetries, propagation effects due to Dione induced density variations in the plasma torus, and phase variations in the outgassing rate due to surface asymmetries on Dione.

References and Notes

1. F. L. Scarf and D. A. Gurnett, Space Sci. Rev. 21, 289 (1977).

2. F. L. Scarf, D. A. Gurnett and W. S. Kurth, Science 204, 991 (1979); D. A. Gurnett, W. S. Kurth and F. L. Scarf, Science 206, 987 (1979).

3. P. Rodriguez, J. Geophys. Res. 84, 917 (1979); F. L. Scarf, W. W. L. Taylor, C. T. Russell, and R. C. Elphic, ibid. 85, 7599 (1980).

4. N. F. Ness et al., Science, this issue.

5. R. R. Shaw and D. A. Gurnett, J. Geophys. Res. 80, 4259 (1975); K. Ronnmark, H. Borg, P. S. Christiansen, M. P. Gough, and D. Jones, Space Sci. Rev. 22, 401 (1978); W. S. Kurth, J. D. Craven, L. A. Frank and D. A. Gurnett, J. Geophys. Res. 84, 4145 (1979).

6. H. S. Bridge et al., Science, this issue.

7. L. A. Frank, B. G. Burek, K. L. Ackerson, J. H. Wolfe, and J. D. Mihalov, J. Geophys. Res. 85, 5695 (1980).

8. G. McK. Allcock, Austr. J. Phys. 10, 286 (1957); C. T. Russell, R. E. Holtzer and E. J. Smith, J. Geophys. Res. 74, 755 (1969); F. L. Scarf, D. A. Gurnett and W. S. Kurth, Science 204, 991 (1979); F. V. Coroniti, F. L. Scarf, C. F. Kennel, W. S. Kurth and D. A. Gurnett, Geophys. Res. Lett. 7, 45 (1980).

9. C. F. Kennel, F. L. Scarf, R. W. Fredricks, J. H. McGehee and F. V. Coroniti, J. Geophys. Res. 75, 6136 (1970); W. S. Kurth, D. D. Barbosa, D. A. Gurnett and F. L. Scarf, Geophys. Res. Lett. 7, 57 (1980).

10. D. A. Gurnett and R. R. Shaw, J. Geophys. Res. 78, 8136 (1973); D. A. Gurnett, ibid. 80, 2751 (1975); W. S. Kurth, D. A. Gurnett and R. R. Anderson, ibid., in press.

11. D. A. Gurnett, L. A. Frank and R. P. Lepping, J. Geophys. Res., 81, 6059 (1976); D. A. Gurnett and L. A. Frank, ibid. 82, 1031 (1977).

12. A. L. Broadfoot et al., Science, this issue.

13. M. L. Kaiser, M. D. Desch, J. W. Warwick and J. B. Pearce, Science 209, 1238 (1980); M. D. Desch and M. L. Kaiser, Geophys. Res. Lett. 8, in press.

14. E. J. Smith et al., Science 207, 407 (1980); M. H. Acuna and N. F. Ness, Science 207, 444 (1980).

15. B. A. Smith et al., Science, this issue.

16. We express our thanks to the entire Voyager team at NASA Headquarters and the Jet Propulsion Laboratory (JPL) for their support. We are especially grateful to R. Poynter for his invaluable assistance and support. We also wish to extend our special thanks to E. Miner and J. Diner for their efforts to arrange the wideband coverage. We are indebted to J. Anderson, P. Jepsen, and G. Garneau for their assistance with the wideband data processing, and to C. Stembridge for his help in solving numerous problems. We also wish to thank H. Bridge, J. Belcher, J. Scudder and N. Ness for providing data in advance of publication and for their helpful discussions. We also acknowledge the outstanding support provided by R. Anderson, R. West, L. Granroth and R. Brechwald in carrying out the data reduction at The University of Iowa. The research at The University of Iowa was supported by NASA through contract 954013 with JPL, through grants NGL-16-001-002 and NGL-16-001-043 with NASA Headquarters and by the Office of Naval Research. The research at TRW was supported by NASA through contract 954012 with JPL.

Figure Captions

Figure 1 An overview of the electric field intensities detected for a 3-day period starting shortly before the inbound shock crossings (S) and ending shortly after the outbound magnetopause crossing (M). Strong plasma wave intensities were observed at the Titan flyby (shown expanded in Figure 2) and through the inner region of the magnetosphere near closest approach. The intense signals in the 3.11-to 56.2-kHz channels around 1200 on 13 November are radio emissions from Saturn.

Figure 2 The top panel shows the equatorial plane projection of the spacecraft trajectory near Titan, and the bottom panel shows the corresponding electric field intensities. The intense low frequency noise suggests the existence of a highly turbulent sheath region extending around Titan. The electron density profile (dashed line) determined from upper hybrid resonance (UHR) emissions shows that a dense plume of plasma extends into the downstream wake, apparently being carried away by the magnetospheric interaction. The question marks indicate uncertainties about the peak densities because of the absence of measurements above 56.2 kHz.

Figure 3 The plasma wave electric field intensities in the region near closest approach. The dashed line gives the approximate electron plasma frequency, f_p, profile derived from a combination of electron plasma oscillations, radio emission propagation cutoffs, and upper hybrid resonance (UHR) emissions. Question marks indicate regions of uncertainty in the profile. The electron gyrofrequency, f_g, profile was obtained from the magnetometer.

Figure 4 A meridian plane plot of the spacecraft trajectory showing the regions of low electron density determined from the electron plasma frequency profile in Figure 3. The highest electron densities were encountered inside of a torus-like region with a north-south thickness of about 4 R_S.

Figure 5 Wideband spectrograms from the points marked A and B in Figure 4. A band of whistler-mode hiss and chorus is evident in both spectrograms at frequencies below about 2 kHz. In the bottom panel the diffuse emissions slightly above the electron gyrofrequency harmonics are electrostatic electron cyclotron waves. The intense bands at about 6 and 9.6 kHz in the top panel are electromagnetic waves propagating in the left-hand ordinary mode at frequencies above the local electron plasma frequency. The plasma frequency, f_p = 2.4 kHz, was determined using the electron density from the plasma instrument.

Figure 6 The top panel shows a representative Saturn radio emission event. The time scale corresponds to one rotation of Saturn. The bottom panel shows the emission probability at 56.2 kHz as a function of the subsolar longitude using the PRA Saturn longitude system (SLS). The absence of a phase shift between the inbound and outbound passes shows that the Saturn rotational control is a temporal (clock-like) effect, with the radiation being emitted in all directions at a certain phase of Saturn's rotation.

Figure 7 A 16-day plot showing the long-term quasi-periodic modulation of the Saturn radio burst intensities. This modulation appears to be controlled by the orbital position of Dione, with the largest intensities occurring as Dione passes through the local morning region of the magnetosphere. The orbital phase angle is measured positive eastward from a plane containing the Sun and the rotational axis of Saturn, with 0° at local midnight.

Figure 8 The radio emission intensity at 56.2 kHz as a function of the subsolar SLS longitude and the Dione orbital phase angle. The strongest emissions occur in the upper left-hand quadrant, when the subsolar SLS longitude is near 90° and Dione is passing through the local morning region of the magnetosphere.

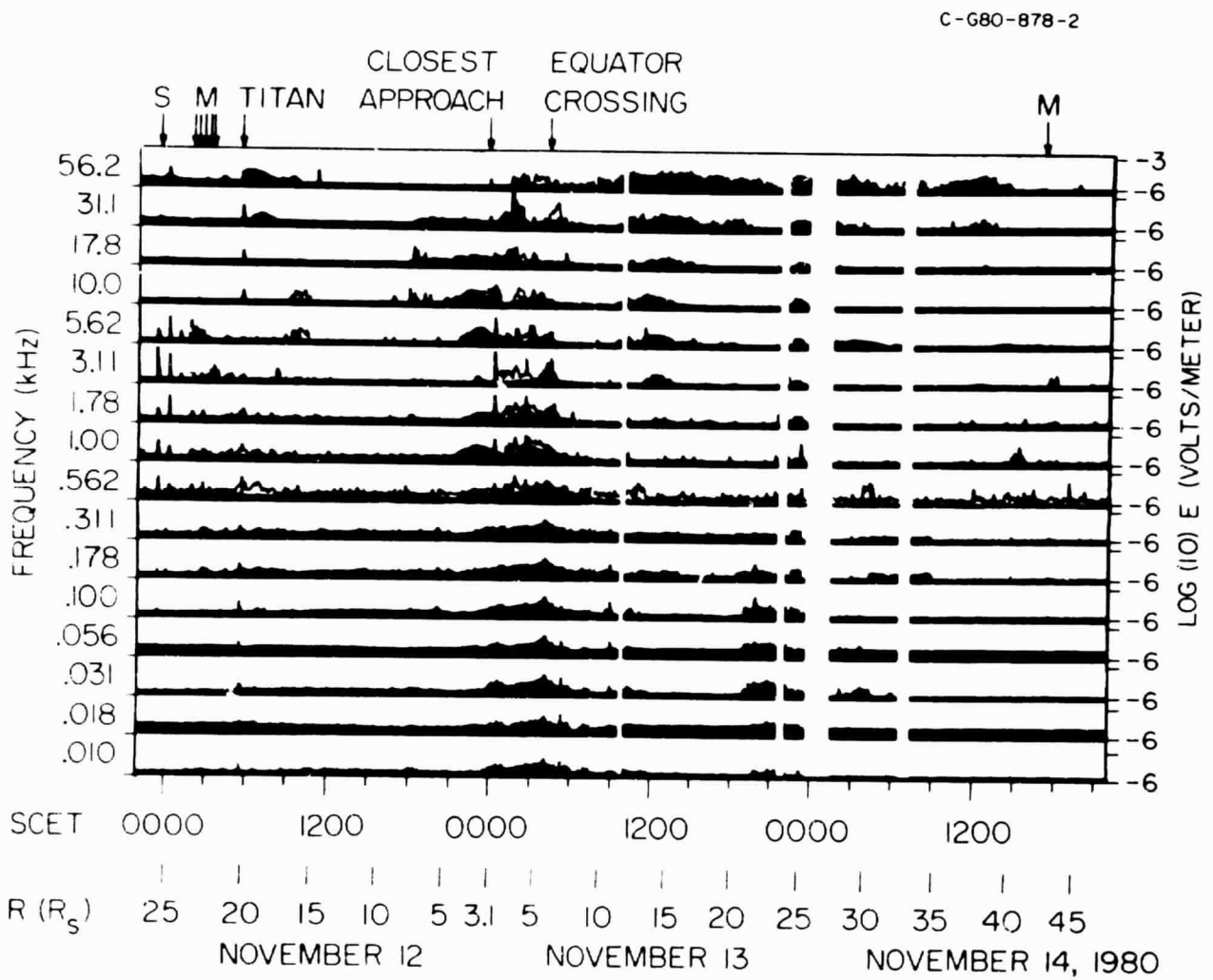
C-G80-878-2
S
M
TITAN
CLOSEST APPROACH
EQUATOR CROSSING
M
56.2
31.1
17.8
10.0
5.62
3.11
1.78
1.00
.562
.311
.178
.100
.056
.031
.018
.010
FREQUENCY (kHz)
-3
-6
LOG (10) E (VOLTS/METER)
SCET 0000 1200 0000 1200 0000 1200
R (Rs) 25 20 15 10 5 3.1 5 10 15 20 25 30 35 40 45
NOVEMBER 12
NOVEMBER 13
NOVEMBER 14, 1980

Figure 1

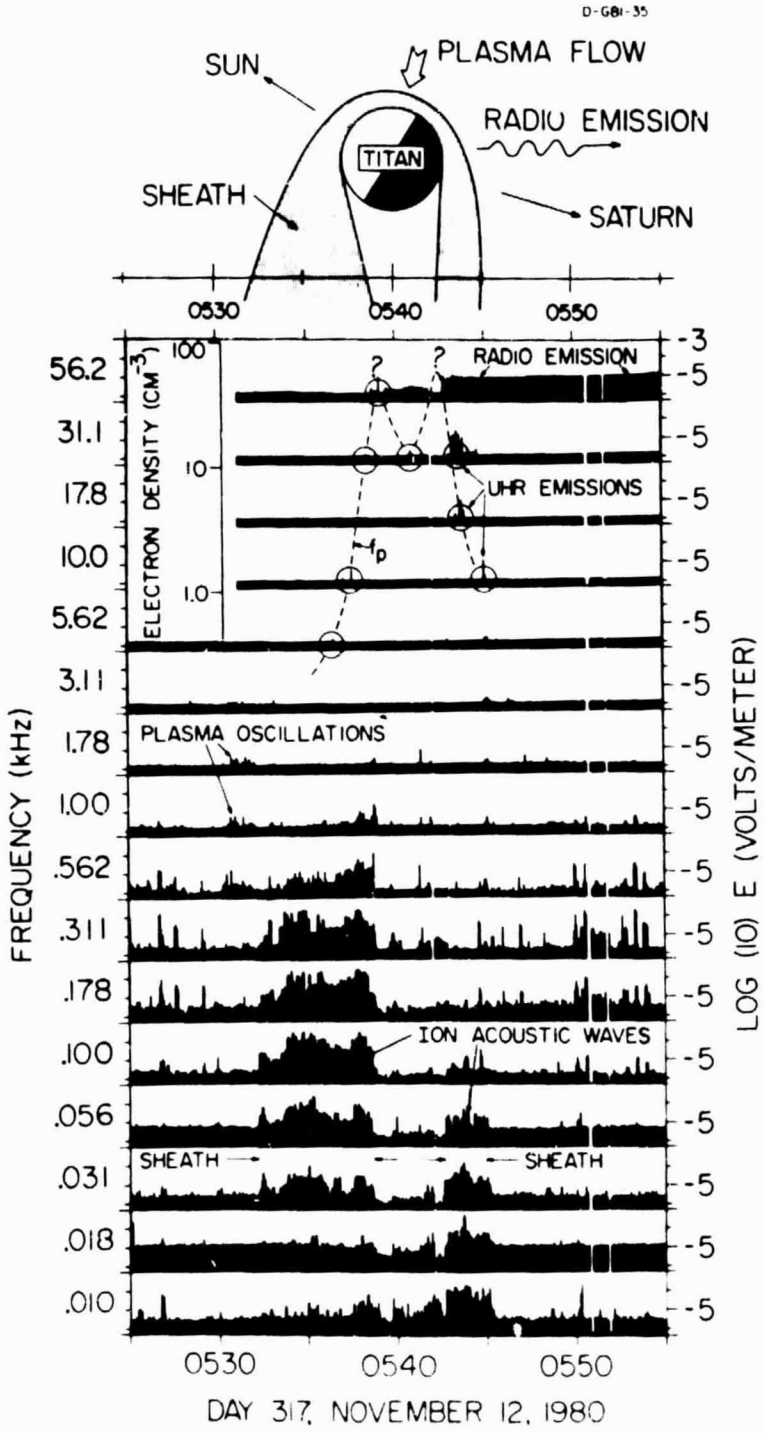
D-G81-35
SUN
PLASMA FLOW
RADIO EMISSION
TITAN
SHEATH
SATURN
0530
0540
0550
ELECTRON DENSITY (CM^{-3})
100
10
1.0
RADIO EMISSION
UHR EMISSIONS
f_p
PLASMA OSCILLATIONS
ION ACOUSTIC WAVES
SHEATH
SHEATH
FREQUENCY (kHz)
56.2
31.1
17.8
10.0
5.62
3.11
1.78
1.00
.562
.311
.178
.100
.056
.031
.018
.010
LOG (10) E (VOLTS/METER)
-3
-5
0530
0540
0550
DAY 317, NOVEMBER 12, 1980

Figure 2

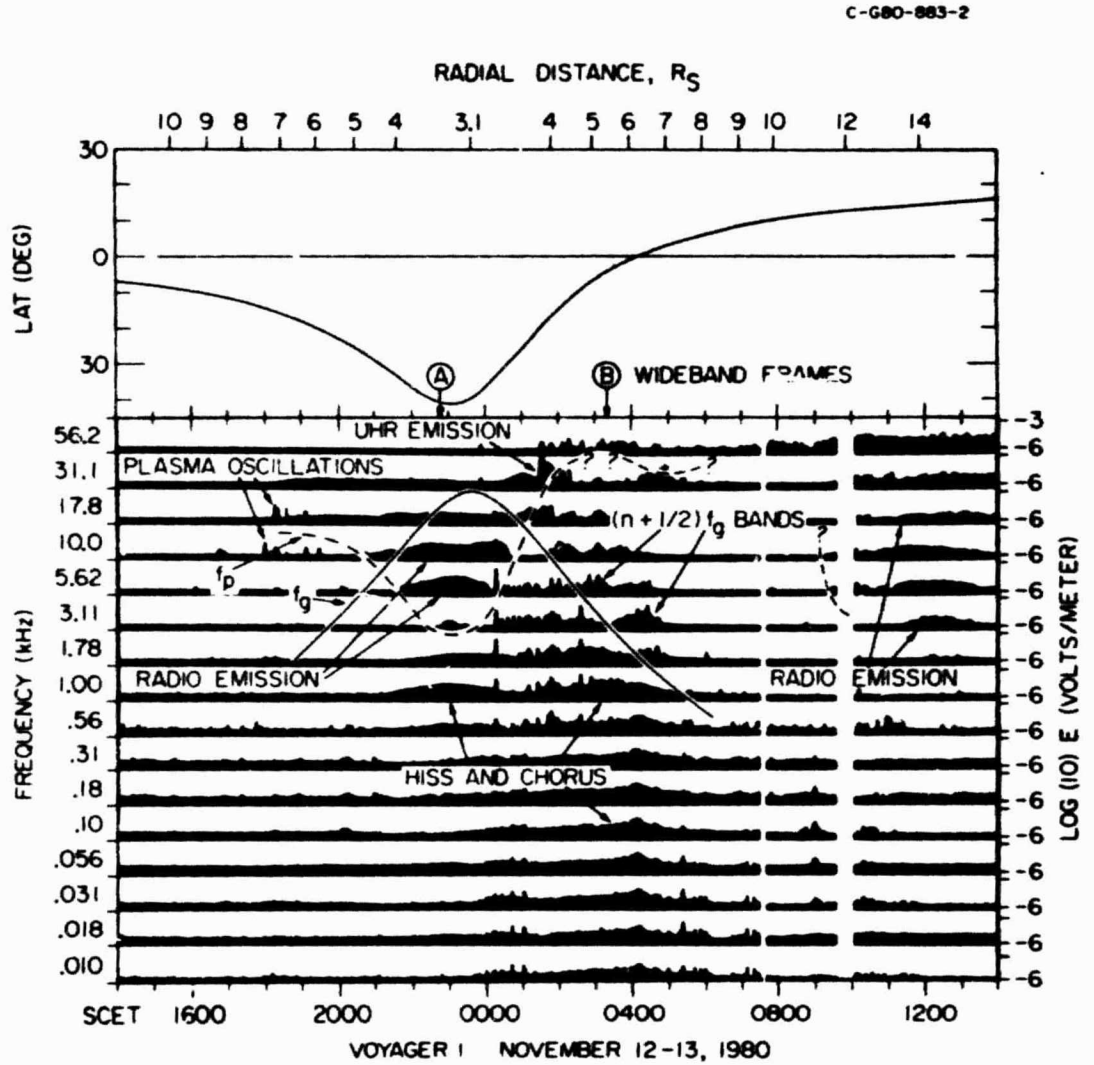
C-G80-883-2
RADIAL DISTANCE, R_S
10 9 8 7 6 5 4 3.1 4 5 6 7 8 9 10 12 14
LAT (DEG)
30
0
30
A
B WIDEBAND FRAMES
UHR EMISSION
PLASMA OSCILLATIONS
(n + 1/2) f_g BANDS
f_p
f_g
RADIO EMISSION
RADIO EMISSION
HISS AND CHORUS
FREQUENCY (kHz)
56.2
31.1
17.8
10.0
5.62
3.11
1.78
1.00
.56
.31
.18
.10
.056
.031
.018
.010
LOG (10) E (VOLTS/METER)
-3
-6
SCET 1600 2000 0000 0400 0800 1200
VOYAGER 1 NOVEMBER 12-13, 1980

Figure 3

A-80-870-3

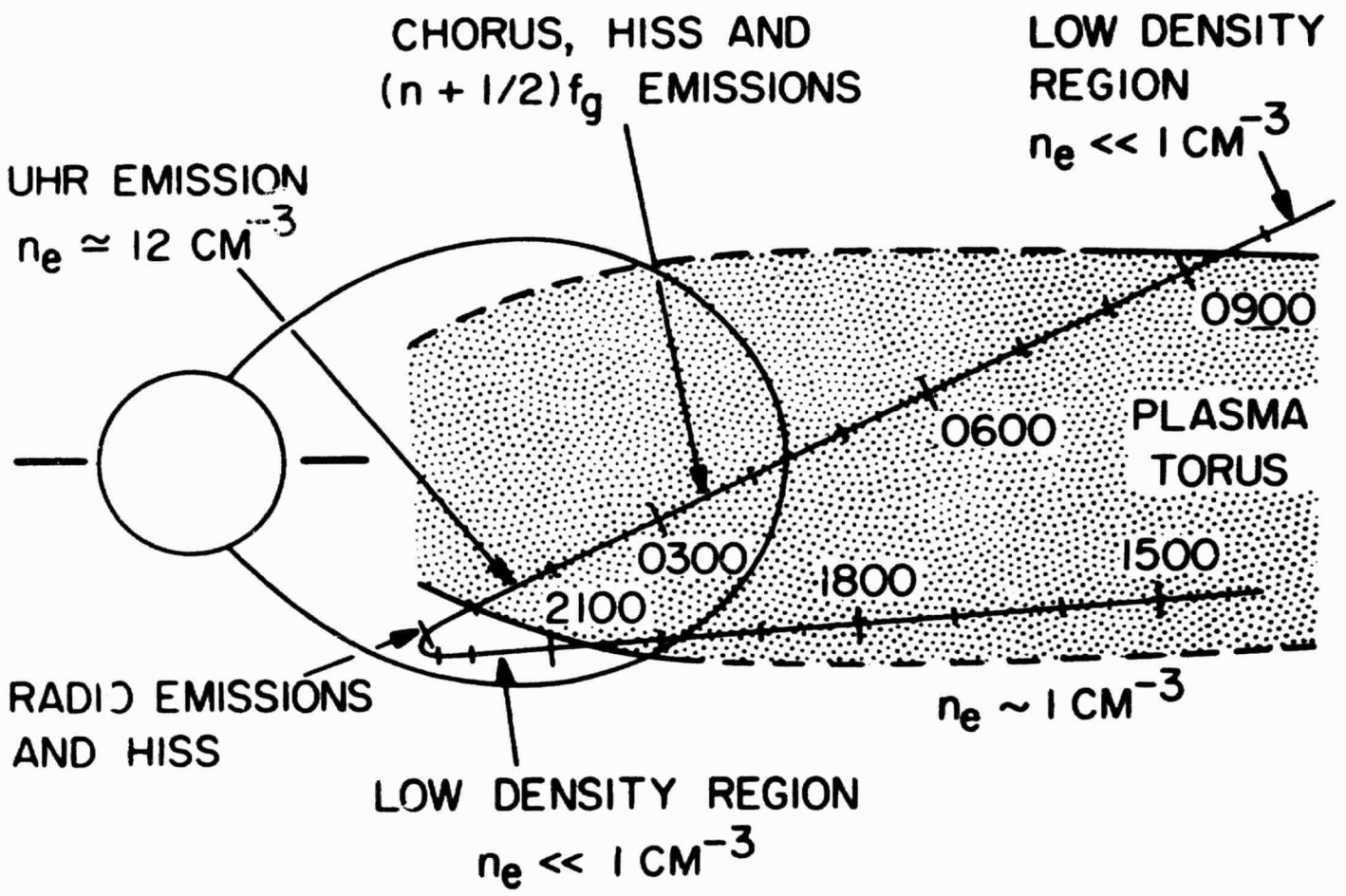

Figure 4

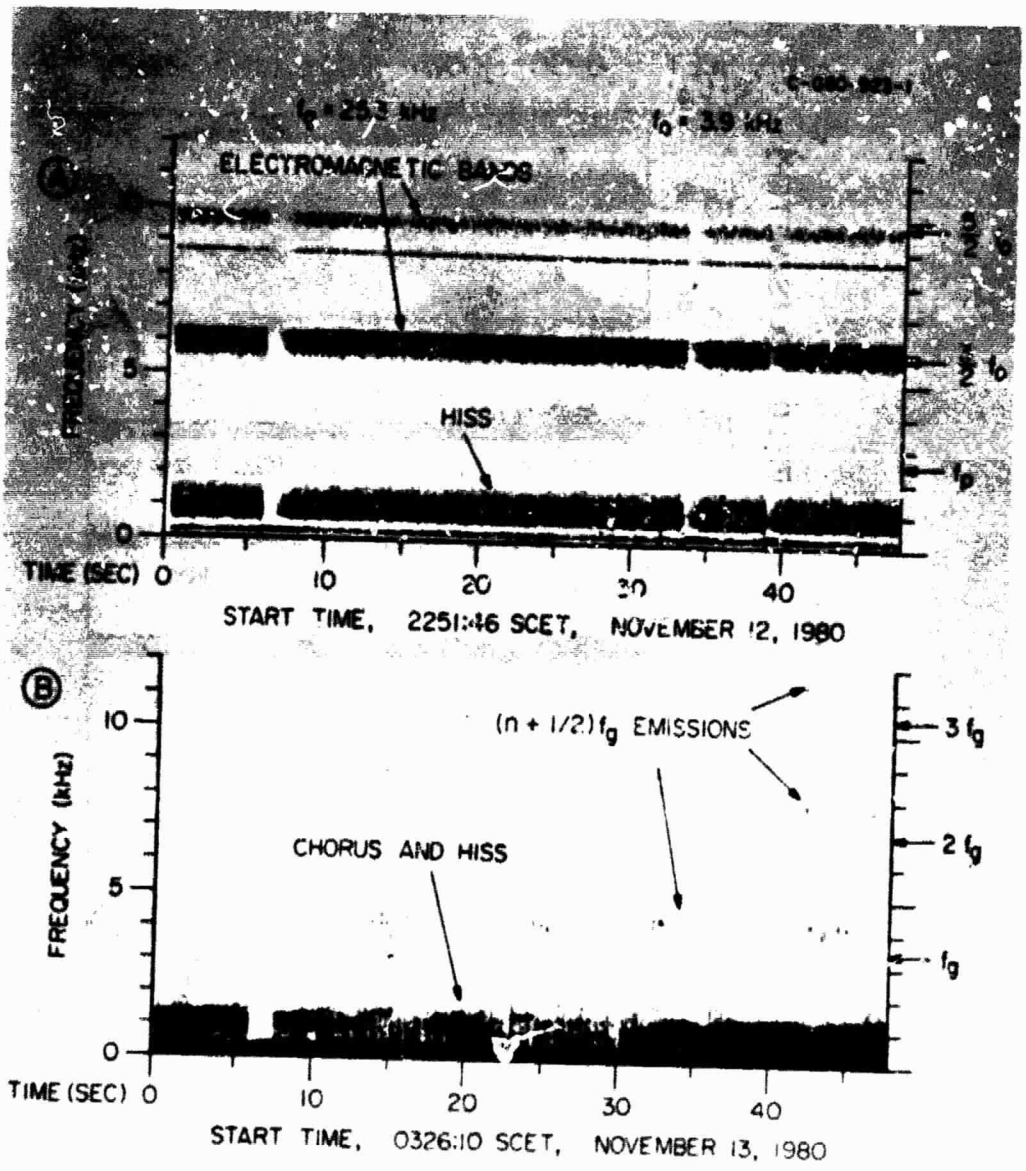

Figure 5

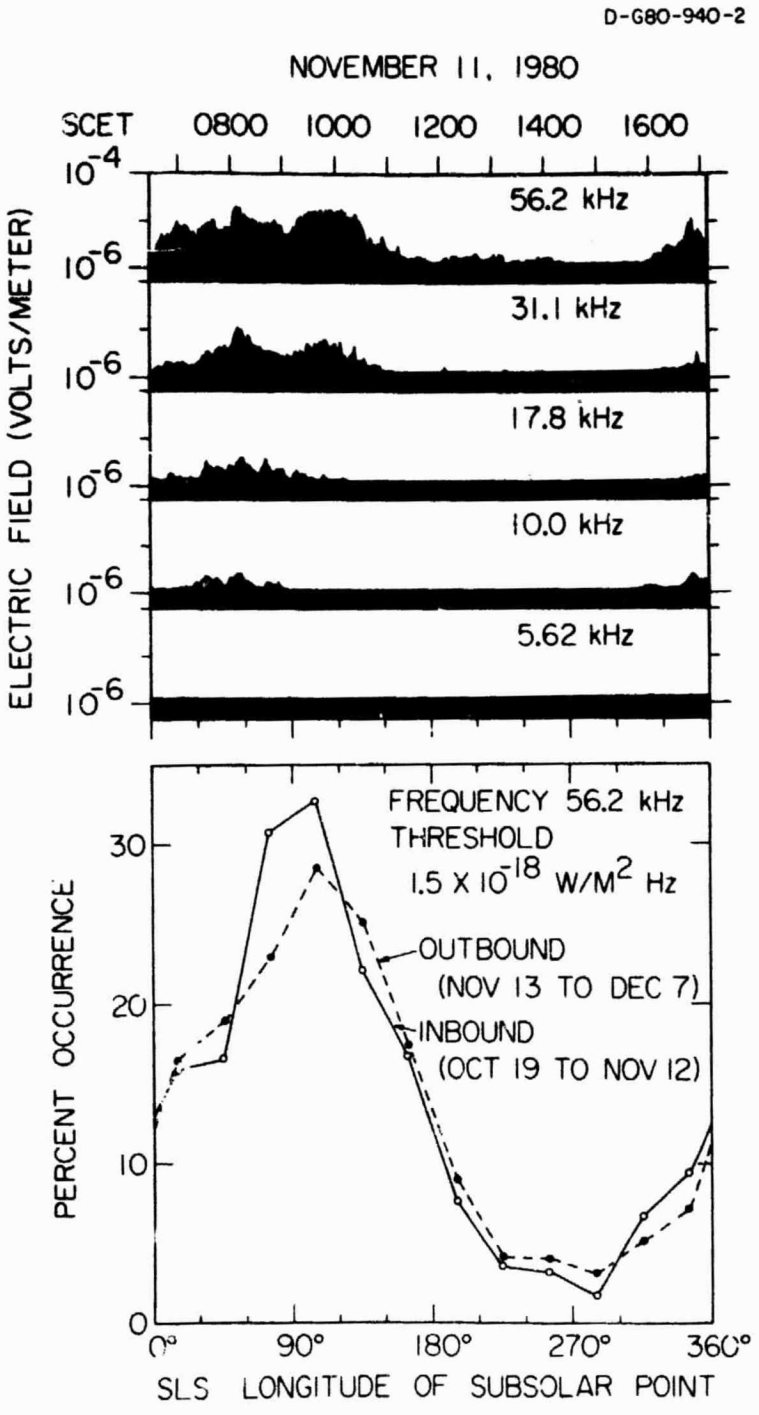
D-G80-940-2
NOVEMBER 11, 1980
SCET
0800
1000
1200
1400
1600
ELECTRIC FIELD (VOLTS/METER)
10^{-4}
10^{-6}
56.2 kHz
31.1 kHz
17.8 kHz
10.0 kHz
5.62 kHz
FREQUENCY 56.2 kHz
THRESHOLD
1.5×10^{-18} W/M^2 Hz
OUTBOUND
(NOV 13 TO DEC 7)
INBOUND
(OCT 19 TO NOV 12)
PERCENT OCCURRENCE
0
10
20
30
0°
90°
180°
270°
360°
SLS LONGITUDE OF SUBSOLAR POINT

Figure 6

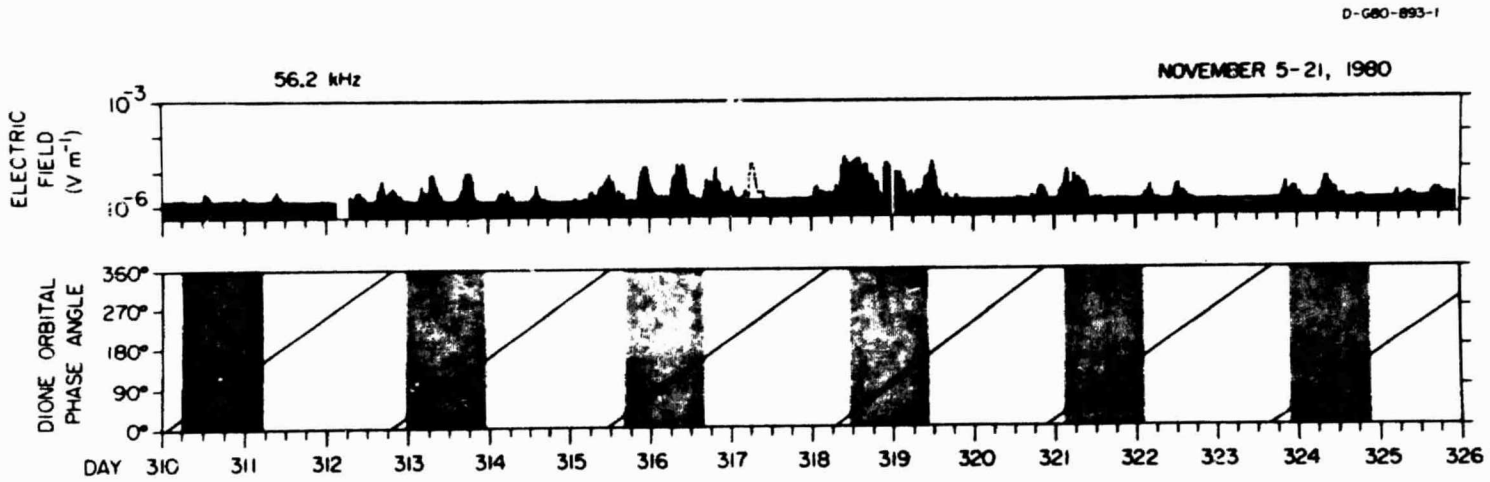
D-G80-893-1
56.2 kHz
NOVEMBER 5-21, 1980
ELECTRIC FIELD (V m⁻¹)
10⁻³
10⁻⁶
DIONE ORBITAL PHASE ANGLE
360°
270°
180°
90°
0°
DAY 310 311 312 313 314 315 316 317 318 319 320 321 322 323 324 325 326

Figure 7

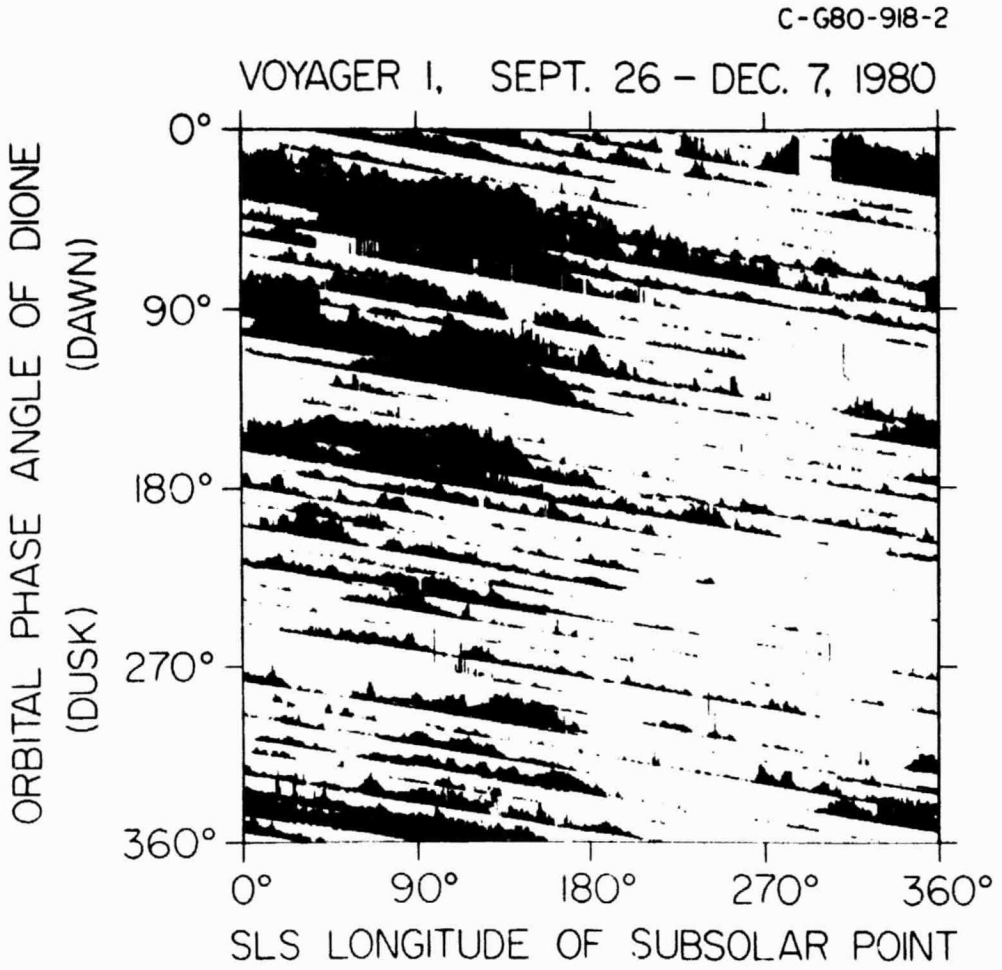

Figure 8